「材料」(Journal of the Society of Materials Science, Japan), Vol. 55, No. 4, pp. 432-437, Apr. 2006
Original Papers

Effects of the Cross-Sectional In-Plane Crystal Orientation on the Structural Strength of Single-Crystal Turbine Vanes †

by

Jinxiang CHEN*, Ryosaku HASHIMOTO**, Yoshitaka FUKUYAMA**, Masahiro MATSUSHITA**, Makoto OSAWA***, Hiroshi HARADA***, Tadaharu YOKOKAWA*** and Toyoaki YOSHIDA****

This paper presents the effects of the cross-sectional in-plane crystal orientation (θ) on the structural strength of single crystal turbine vanes using the finite element method (FEM). The material of the turbine vanes is the single crystal superalloy TMS-75. The obtained results show that the elastic constant matrix (c'_{44}) changes were by above 60% due to the orientation variation ($0^\circ < \theta < 90^\circ$). The dependency of the structural strength of the turbine vane on the crystal orientation was calculated using von Mises stress equation. The strength of the turbine vane was strongly related to θ, and also related to the model shape and load. This influence becomes more significant near the leading edge of the turbine vane where it is most likely to fracture.

Key words : *Anisotropy, Thermal Stress, Creep, Single-Crystal, TMS-75, Orientation, Von Mises Stress*

1 Introduction

The thermal efficiency of gas turbine is an important factor that strongly affects the CO_2 emission reduction and the prevention of global warming, and in order to make significant improvements in this efficiency, the increase in the turbine inlet temperature (TIT) is required. For this reason, Ni-base single crystal (SC) superalloys were developed for the applications in gas turbines in order to achieve increasingly higher operating temperatures.[1)]

The gas turbine blades and vanes made of SC superalloy show complex mechanical properties, because of its anisotropic properties. On the actual blades and vanes, the orientation of [001] in the radial direction is the well-established manufacturing method. However, the in-plane crystal orientation is conventionally not controlled. The effect of elastic anisotropy is being researched through the comparison between the isotropic and the anisotropic analyses[2)~4)] and thermal stress analysis of SC during growth.[2), 5)] Anisotropy in multiaxial creep and fatigue has also been investigated.[6)~10)] The elastic matrix components of face-centred-cubic SC have been expressed by Miyazaki et al in terms of an arbitrary Cartesian coordinate system.[11)]

On the other hand, it is difficult to evaluate structural strength of turbine blades and vanes, because of their complicated shapes and working environment. Simple models as cylinder and simple thermal loads have been reported in most published papers.[5), 7), 12)] Very few attempts have been made at the structural strength of SC turbine blades and vanes under the real shapes[13)] and operating environment. However, as the SC turbine blades and vanes are expensive, it is desired to make the best use of the anisotropy reconcile with the operating environment. The structural strength characteristics, and its dependency on the crystal orientation should be investigated. In this paper, the effects of the in-plane crystal orientation on the structural strength of turbine vanes were investigated for broad applications of the SC in the gas turbine industry.

2 Analytical Modeling Descriptions

The analytical model is of a 1st stage gas turbine vane of 1400℃ class and the material used was SC superalloy TMS-75. Figure 1 (a) shows the analytical model of a turbine vane. In Fig. 1, the dimensionless parameter H corresponds to the vane height, where H0% and H100% represents the hub and tip of the turbine vane, respectively. In the same manner, the dimensionless parameter L represents the external surface position as shown in Fig. 1 (b). The leading edge and trailing edge are located at 0% and 100% positions, respectively. The pressure side was set as negative and the suction side as positive. X, Y and Z-axis represent the axial, circumferential and radial direction of the vane respectively. The crystal orientation relative to the basis is described by θ, the angle between SC [100] direction and X-axis, in which the Z-axis coincides with the [001] crystallographic direction as shown

† Received July 14, 2005
* Member: Aeronautical Envi. Tech. Center, Japan Aerospace Exploration Agency, Jindaiji, Chofu, 182-8522 Japan
** Aeronautical Envi. Tech. Center, Japan Aerospace Exploration Agency, Jindaiji, Chofu, 182-8522 Japan
*** Materials Eng. Lab., High Temperature Materials Group, National Inst. for Materials Sci., Sengen, Tsukuba, 305-0047 Japan
**** Dept. of Mech. Systems Eng., Graduate School of Tech., Tokyo Univ. of Agriculture and Tech., Naka-cho, Koganei, 184-8588 Japan

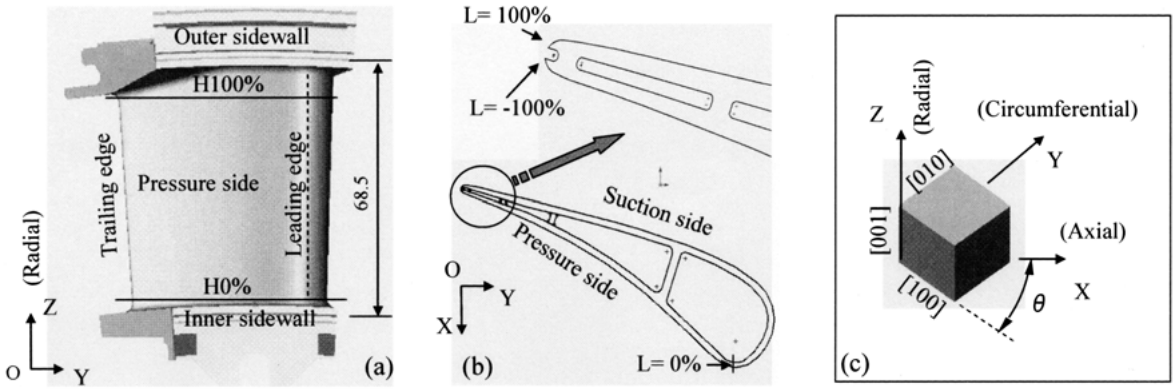

Fig. 1 Analysis model (a), normalized position in cross-section of vane (b) and single crystal direction with θ degree (c).

in Fig. 1 (c). When considered in terms of the simple cylindrical coordinate system, the matrix components of SC are known to be dependent on θ and varies cyclically with a period of 90°.[2), 5)] Similar variations were expected in this study, thus, 6 cases were considered with various values of θ in the range from 0° to 75° at 15° intervals. The thermal load and gas pressure were imitating those in the operating condition of a 1400℃ class gas turbine,[14)] and the temperature distribution on the external surfaces of the turbine vane at different cross-sections is shown in Fig. 2. Analysis was done with Nastran for Windows Visual 2003. The geometry of the vane was meshed by tetrahedral elements, with 106042 elements and 33318 nodes (see Fig. 3). As shown in Fig. 3, the nodes on the surface of the outer and inner sidewalls were constrained.[4)] The analysis of creep rupture life and data processing were carried out by an existing evaluation system.[14)]

3 Formulation, FEM Analysis Results and Discussion

3.1 Formulation

For cubic single crystals, when the X, Y and Z-axes coincide with the crystallographic axes (Fig. 1 (c), $\theta = 0°$), there are only three independent elastic constants c_{11}, c_{12} and c_{44} as expressed in Eq. (1).[11), 15)]

$$\begin{Bmatrix}\sigma_1\\ \sigma_2\\ \sigma_3\\ \sigma_{12}\\ \sigma_{23}\\ \sigma_{31}\end{Bmatrix} = \begin{bmatrix} c_{11} & c_{12} & c_{12} & 0 & 0 & 0\\ & c_{11} & c_{12} & 0 & 0 & 0\\ & & c_{12} & 0 & 0 & 0\\ & & & c_{44} & 0 & 0\\ & Sym. & & & c_{44} & 0\\ & & & & & c_{44}\end{bmatrix} \begin{Bmatrix}\varepsilon_1\\ \varepsilon_2\\ \varepsilon_3\\ \varepsilon_{12}\\ \varepsilon_{23}\\ \varepsilon_{31}\end{Bmatrix} \quad (1)$$

Here, indices 1, 2 and 3 indicate the crystallographic axes of the material (SC). For practicality, Eq. (1) is described by the Eq. (1a).

$$\{\sigma\}_{123} = [A]\{\varepsilon\}_{123} \quad (1a)$$

When $\theta \neq 0°$ as shown in Fig. 1 (c), direction cosine from the crystallographic axes to Cartesian coordinate is described as Eq. (2).

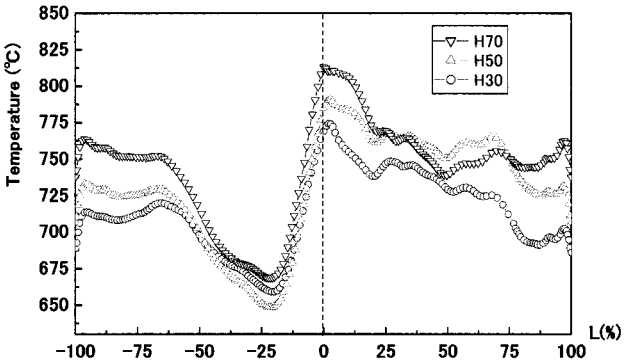

Fig. 2 Temperatures of different cross-sections on the external surfaces of the turbine vane.

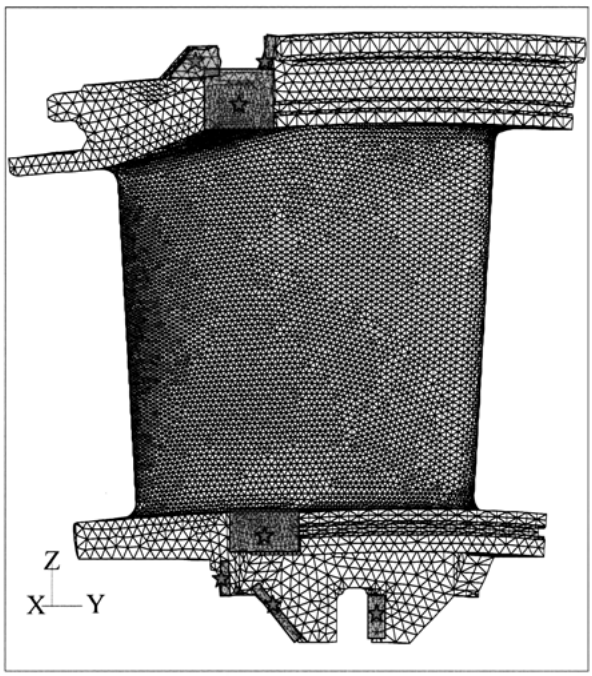

Fig. 3 The mesh distribution and boundary condition. The DOF of the nodes on the surfaces (☆) were partly constrained.

$$g=\begin{bmatrix}\cos\theta & \sin\theta & 0\\ -\sin\theta & \cos\theta & 0\\ 0 & 0 & 1\end{bmatrix} \tag{2}$$

In this case, the elastic constant matrix [A'] in Cartesian coordinate is determined by the coordinate transformation rule of Eq. (3).[16)]

$$[A']=[T][A][T]^T \tag{3}$$

Here, [T] is the coordinate transformation matrix[17), 18)] and is formulated as Eq. (3a).

$$[T]=\begin{bmatrix}\cos^2\theta & \sin^2\theta & 0 & \sin 2\theta & 0 & 0\\ \sin^2\theta & \cos^2\theta & 0 & -\sin 2\theta & 0 & 0\\ 0 & 0 & 1 & 0 & 0 & 0\\ -\sin 2\theta/2 & \sin 2\theta/2 & 0 & \cos 2\theta & 0 & 0\\ 0 & 0 & 0 & 0 & \cos\theta & -\sin\theta\\ 0 & 0 & 0 & 0 & \sin\theta & \cos\theta\end{bmatrix} \tag{3a}$$

Then the elastic constant matrix can be expressed as Eq. (4).

$$\begin{Bmatrix}\sigma_x\\ \sigma_y\\ \sigma_z\\ \sigma_{xy}\\ \sigma_{yz}\\ \sigma_{zx}\end{Bmatrix}=\begin{bmatrix}c'_{11} & c'_{12} & c_{12} & c'_{14} & 0 & 0\\ & c'_{11} & c_{12} & -c'_{14} & 0 & 0\\ & & c_{11} & 0 & 0 & 0\\ & & & c'_{44} & 0 & 0\\ & Sym. & & & c_{44} & 0\\ & & & & & c_{44}\end{bmatrix}\begin{Bmatrix}\varepsilon_x\\ \varepsilon_y\\ \varepsilon_z\\ \varepsilon_{xy}\\ \varepsilon_{yz}\\ \varepsilon_{zx}\end{Bmatrix} \tag{4}$$

with

$$c'_{11}=c_{11}-\sin^2 2\theta\cdot c_- \tag{4a}$$
$$c'_{12}=c_{12}+\sin^2 2\theta\cdot c_- \tag{4b}$$
$$c'_{14}=-\sin 4\theta\cdot c_-/2 \tag{4c}$$
$$c'_{44}=c_{44}+\sin^2 2\theta\cdot c_- \tag{4d}$$
$$c_-=(c_{11}-c_{12}-2c_{44})/2 \tag{4e}$$

Equation (4) is essentially in accordance with the results of Miyazaki et al.[11)] Values of c_{11}, c_{12} and c_{44} on the SC superalloy TMS-75 were shown in Table 1. To discuss the effects of θ on the elastic constant, the relationship curves between c'_{11}, c'_{12}, c'_{44}, c'_{14} and θ were produced as shown in Fig 4 (a), by using the values of c_{11}, c_{12}, c_{44} for a temperature of 700℃, which is close to the average temperature of the external and inner surfaces of the turbine vane (blade). The variation of c'_{11}, c'_{12}, c'_{44} with their values at $\theta=0^\circ$ as the reference, is shown in Fig. 4 (b). From Fig. 4, it is clear that c'_{11}, c'_{12} and c'_{44} strongly depend on θ in the sine function with a period of 90°, and the maximum changes were by over 30%, 45% and 60%, respectively.

Next, the effects of the crystal orientation θ on von Mises stress were investigated using Eq. (5) :

$$\sigma=\sqrt{\left[(\sigma_x-\sigma_y)^2+(\sigma_y-\sigma_z)^2+(\sigma_z-\sigma_x)^2\right]/2+3\left(\tau_{xy}^2+\tau_{yz}^2+\tau_{zx}^2\right)} \tag{5}$$

Equation (5) can be rewritten as Eq. (6) through Eq. (4).

$$\sigma=\sqrt{\sigma_0+\sigma_\theta} \tag{6}$$

with

$$\sigma_0=(c_{11}-c_{12})^2\,\varepsilon_a/2+3c_{44}^2\,\varepsilon_b \tag{7}$$
$$\varepsilon_a=(\varepsilon_y-\varepsilon_x)^2+(\varepsilon_x-\varepsilon_z)^2+(\varepsilon_x-\varepsilon_y)^2 \tag{7a}$$
$$\varepsilon_b=\varepsilon_{xy}^2+\varepsilon_{yz}^2+\varepsilon_{zx}^2 \tag{7b}$$
$$\sigma_\theta=3c_+c_-\left(\varepsilon_c\sin^2 2\theta-\varepsilon_a\sin 4\theta\right) \tag{8}$$
$$\varepsilon_c=\varepsilon_{xy}^2-(\varepsilon_x-\varepsilon_y)^2 \tag{8a}$$
$$\varepsilon_d=(\varepsilon_x-\varepsilon_y)\varepsilon_{xy} \tag{8b}$$
$$c_+=(c_{11}-c_{12}+2c_{44})/2 \tag{8c}$$

From Eqs. (6) to (8), σ is not only dependent on θ, but also related to many factors such as the elastic constant

Table 1 Values of elastic constants of the SC superalloy TMS-75.

Temperature	c_{11} (GPa)	c_{12} (GPa)	c_{44} (GPa)
400℃	231.8	149.9	120.6
500℃	227.8	148.9	117.2
600℃	223.9	147.9	113.7
700℃	219.9	146.9	110.1
800℃	216.0	146.0	106.3
900℃	212.0	145.0	102.4
1000℃	208.0	144.0	98.5

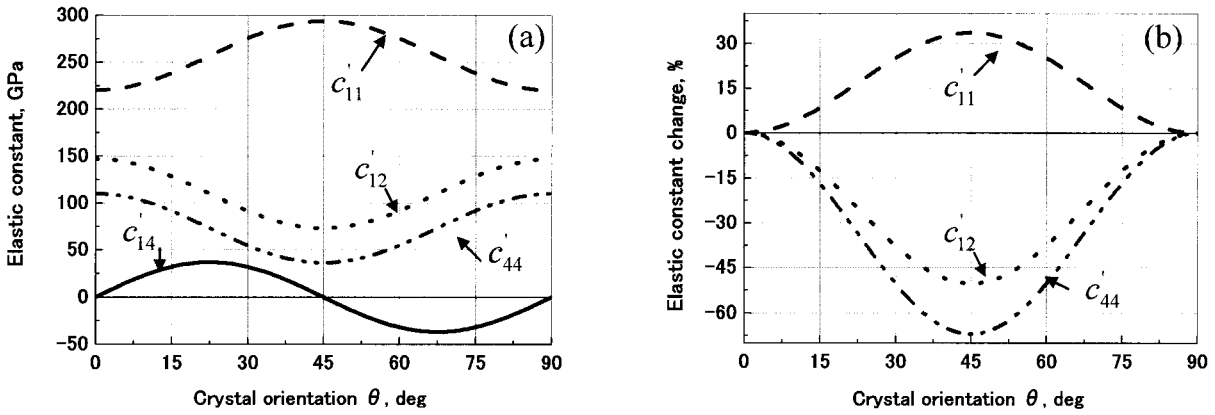

Fig. 4 Relations between the elastic constants and θ, (a) absolute value, (b) relative value.

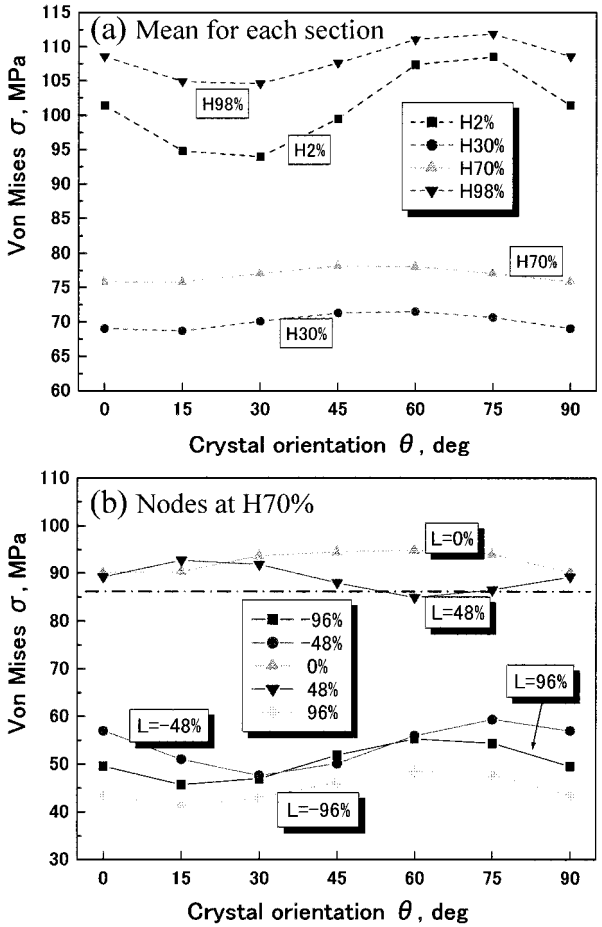

Fig. 5 Distribution of von Mises stress, the means of H and L (see Fig. 1 (b)).

of material, thermal environment, gas pressure and model shape. The FEM method was used to analyze the effects of θ on the structural strength, because of the consideration required for the complex shape and loads of the vane.

3.2 Results and Discussion

The anisotropy of the creep deformation and plastic deformation are not considered as an initial stage of the research, and the structural strength is investigated using the parameter of the von Mises stress and a creep rupture time calculated by the Larson Miller curve as reported.[4)]

3.2.1 Von Mises Stress First, the variation of stress in the turbine vane with θ in the range of 0° to 90° was studied. Figure 5 (a) shows the average stress of the 101 points which uniformly located on the external surfaces of the turbine vane in four different cross-sections; H2%, H30%, H70%, and H98%. There were cases where the average stress of each surface depended strongly on θ, such as at H2%, however there were also cases, such as at H70% where it was unaffected. The relationship between nodal stress and θ for the position H70% of the vane is shown in Fig. 5 (b). It shows that the nodal stress is strongly dependent on θ in the cross-section at H70%. In other words, in general von Mises stress is dependent on θ. In addition, Miyazaki et al reported that a cylindrical model subjected to two-dimensional thermal loading has a symmetrical stress distribution with a cyclical period of 90°.[2),5)] In the case of a vane, the von Mises stress cyclic variation has a period of 90° in terms of θ, but, does neither have simple sine functions as the c'_{11} and c'_{12} nor symmetrical distributions, because the shape and the loading of the vane are not symmetrical.

The stress difference between the cases of $\theta = 0°$ and 45° were examined. Nodal stresses in three different cross-sections (H10%, H50%, H90%) are shown in Fig. 6. The von Mises stress differences are normalized by the

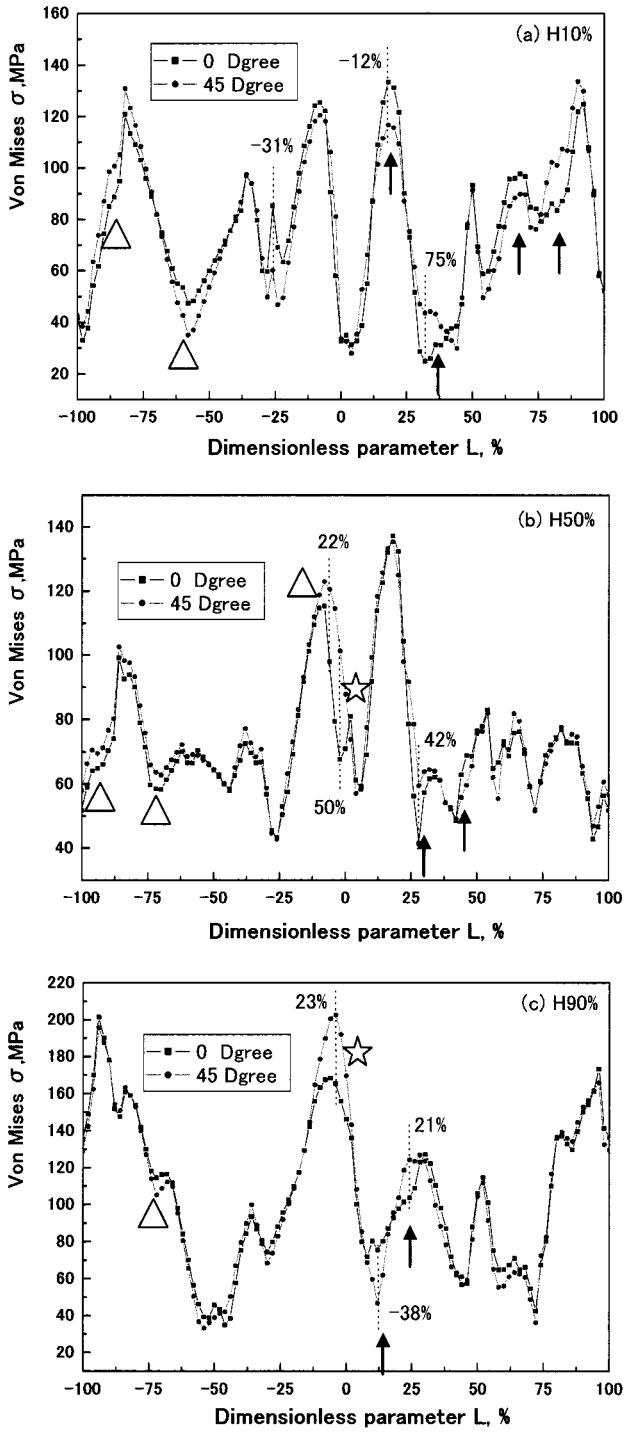

Fig. 6 Distribution of von Mises stress of the nodes in different cross sections for the cases of $\theta = 0°$ and 45°.

stress for $\theta = 0^\circ$, shown in the figure in % unit. From Fig. 6, the difference in von Mises stress between $\theta = 45^\circ$ and $\theta = 0^\circ$ exceeds ±20% on more than one occasion. The extreme values of the von Mises stress variation are 75% and –38% as shown in Fig. 6 (a) and (c), respectively. The peaks and troughs are located at the leading edge (Fig. 6, ☆), suction side (Fig. 6, ↑) and pressure side (Fig. 6 (b), (c) : △) for each cross-section. But they are mainly near the leading edge (Fig. 6, L = –25% ~ +25%). In this study, only three cross-sections in the cases of $\theta = 0^\circ$ and 45° were compared, and it is expected that the differences in von Mises stress will become greater as the number of the investigated cross-sections and θ values increase.

3.2.2 Creep Rupture Life Creep rupture life t_r is estimated by Eq. (9).

$$t_r = 10^{(P_f - TC)/T} \tag{9}$$

where, T is absolute temperature (K), C is constant (20), and P_f is the Larson Miller parameter. P_f is decided by the Larson Miller curve in Fig. 7, which is in accordance with the von Mises stress obtained by FEM analysis. Strictly speaking, anisotropy of the Larson Miller curves of the SC superalloys should be considered, but in this analysis, the Larson Miller curve of the SC superalloys with [001] was used for all the direction as an approximation. The approximation is applied, because data of creep anisotropy is limited, and it seems to us difficult to obtain the anisotropy of the Larson Miller curves from the limited data ever published. In Fig. 7, the points are experimental values and the broken line is the extrapolation.

The relationship between θ and the creep rupture life with respect to the mean value for each cross-section and the nodes at H70% are shown in Fig. 8 (a), (b), respectively. Since the same temperature applies to all cases in this study, the creep rupture life is strongly dependent on P_f. Therefore, the creep rupture life is reduced when von Mises stress is high, and the creep rupture life of the vane depends on θ.

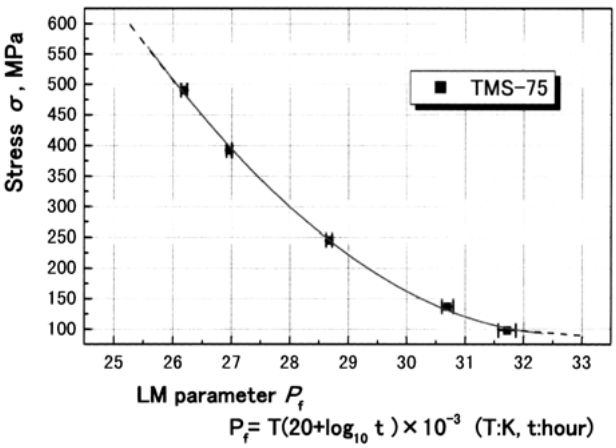

Fig. 7 LM curve of SC superalloy TMS-75.

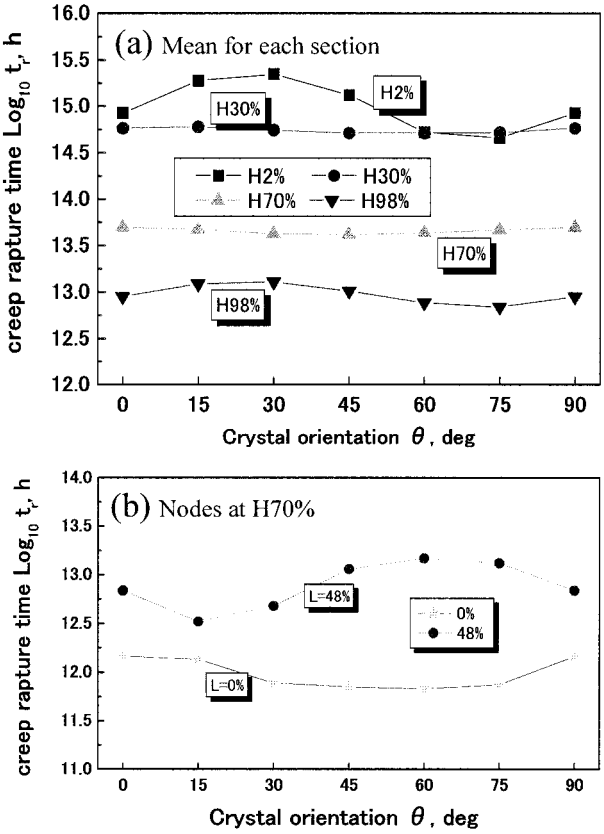

Fig. 8 Creep rupture time distribution of vane.

In order to discuss the change in creep rupture life, the average values of $\mathrm{Log}_{10}\ t_r$ were calculated for the pressure side, suction side and leading edge separately. The change in the creep rupture life Δt was expressed in Eq. (10), in terms of the maximum $t_{\max}$, minimum $t_{\min}$ of the 6 cases with various θ values and $t_{\theta 0}$ of the case $\theta = 0^\circ$ that were considered in this study.

$$\Delta t(\%) = \left(10^{t\max} - 10^{t\min}\right)/10^{t\theta 0} \times 100 \tag{10}$$

From the result calculated by Eq. (10), Table 2 shows that the change in the creep rupture life with θ was more than 20% for the pressure and suction sides of the vane, and a large change was found for the leading edge over 70%. Thus, the creep rupture life strongly depended on θ.

From the results, it is clear that the strength of the SC superalloy turbine vane is influenced strongly by the in-plane crystal orientation and also by other factors such as the model shape and load. This dependency is especially significant near the leading edge. Therefore, these differences cannot be ignored, and careful considerations are required for the model shape and the load in the design of SC superalloy turbine vanes.

Table 2 Variation of creep rapture time normalized by that with $\theta = 0^\circ$(%).

Object	Pressure	Suction	Leading
Vane	28	21	71

4 Conclusions

In this paper the effects of the cross-sectional in-plane crystal orientation on the structural strength of the gas turbine vane of 1400℃ class were investigated using the FEM analysis. The material of the turbine was the single-crystal superalloy TMS-75. The results obtained in present work are :

(1) Some of the elastic constants in the expression for the model were sine function of θ with a period of 90°. Maximum variations of c'_{11}, c'_{12}, c'_{44} were by over 30%, 45% and 60% respectively for θ of 0 to 90 degree.

(2) The von Mises stress dependency on θ was examined. It was not only dependent on θ but related to many factors such as the elastic constant of material, thermal environment, gas pressure and model shape. The dependency of the structural strength of the vane on the crystallographic orientation was found to be complex.

(3) It was clear from the FEM analysis that the effects of θ on the structural strength of the turbine vane are particularly strong near the leading edge where it is mostly prone to fracture.

In the future, the effects of the crystal orientation, model shape and load on the structural strength will be estimated in more detail, and turbine blades will also be investigated. Also the anisotropy of creep deformation and the plastic deformation should be considered in the next step of the research.

This research is a part of High Temperature Materials 21 Project of the National Institute for Materials Science, Japan. We would like to express our gratitude to Toshio Nishizawa of Japan Aerospace Exploration Agency, Shijie Guo of Ebara Research Co. Ltd and Yomei Yoshioka of Toshiba Corporation for their valuable comments.

References

1) H. Harada and M. Okaxaki “High temperature strength of NI-based superalloys and coatings for advanced gas turbines”, Journal of the Society of Materials Science, Japan, Vol.51, No.7, pp.836-842 (2002).

2) N. Miyazaki, H. Uchida, S. Hagihara, T. Munakata and T. Fukuda, “Thermal Stress Analysis of Bulk Single Crystal during Czochralski Growth : Comparison between Anisotropic Analysis and Isotropic Analysis”, JSME International Journal Series A, Vol.57, No.536, pp.858-863 (1991).

3) J. C. Lambropoulos, “The Isotropic assumption during the Czochralski Growth of Single Semiconductors Crystals”, Journal of Crystal Growth, Vol.84, No.3, pp.349-358 (1987).

4) J. Chen, A. Ogawa, R. Hashimoto, T. Yoshida, T. Nishizawa, Y. Fukuyama, T. Yokokawa and H. Harada, “Structural Strength Change by Single Crystallization of Turbine Blades and Vanes”, Journal of the Society of Materials Science, Japan, Vol.54, No.3, pp.251-256 (2005).

5) N. Miyazaki, H. Uchida, S. Hagihara, T. Munakata and T. Fukuda, “Thermal Stress Analysis of Bulk Single Crystals during CZ Growth : Anisotropic Effects in Various Single Crystals” JSME International Journal Series A, Vol.58, No.554, pp.1942-1946 (1992).

6) N. Ohno, T. Mizuno, H. Kawaji and I. Okada, “Multiaxial creep of a nickel-base directionally solidified alloy : anisotropy and simulation”, Acta Materialia, Vol.40, No.3, pp.559-567 (1992).

7) N. Ohno and T. Takeuchi, “Anisotropy in multiaxial creep of nickel-base single crystal superalloy CMSX-2 (experiments and identification of active slip systems)”, JSME International Journal Series A, Vol.37, No.2, pp.129-137 (1994).

8) M. Okazaki, T. Hiura and T. Suzuki, “Nucleation of Cellular Colonies in Single Crystal Ni-Based Superalloy Subjected to Previous Damage and Influence on High Temperature Fatigue Strength”, Journal of the Society of Materials Science, Japan, Vol.50, No.2, pp.94-100 (2001).

9) N. Hiyoshi and M. Sakane, “Tension-Torsion Multiaxial Creep-Fatigue for CMSX-2 Nickel Base Single Crystal Superalloy”, Journal of the Society of Materials Science, Japan, Vol. 50, No.2, pp.137-143 (2001).

10) M. Yamamoto, A. Nitta and T. Ogata, “Evaluation of Crack Initiation and Propagation Lives from Internal Defects and Lower Limit of Failure Life in High Temperature Fatigue on Ni-Based Single Crystal Superalloy”, Journal of the Society of Materials Science, Japan, Vol.50, No.5, pp.510-515 (2001).

11) N. Miyazaki, S. Hagihara and T. Munakata, “Elastic constant matrix required for thermal stress analysis of bulk single crystals during czochralski growth”, Journal of Crystal Growth, Vol.106, pp.149-156 (1990).

12) A. S. Jordan, “A Thermoelastic Analysis of Dislocation Generation in Pulled GaAs Crystals”, The Bell System Technical Journal., Vol.59, pp.593-636 (1980).

13) N. K. Arakere and G. Swanson, “Effect of Crystal Orientation on Fatigue Failure of Single Crystal Nickel Base Turbine Blade Superalloys”, Journal of Engineering for Gas Turbines and Power, Vol.124, No.1, pp.161-176 (2002).

14) J. Chen, A. Ogawa, R. Hashimoto and T. Yoshida, “Interface Construction for Thermal Stress Analysis in Virtual Turbine and Stress Evaluation”, Journal of the Gas Turbine Society of Japan, Vol.32, No.1, pp.34-39 (2004).

15) C. M. Zener, “Elasticity and anelasticity of metals”, pp.7-22 (1948) The University of Chicago Press.

16) K. Washizu, I. Miyamoto, Y. Yamada, Y. Yamamoto and T. Kawai, “Finite Element Method Handbook, II applied compilation”, pp.368-375 (1983) The Baifukan Press.

17) N. Noda, Y. Tanigawa, N. Sumi and T. Tsuji, “Fundamental Elastic Mechanics”, pp.6-25 (1988) The Nisshin Publication Press.

18) M. Zako and K. Matsumoto, “Behavior Analysis of Composite Material”, pp.14-21 (1998) Tokyo, Asakura book store.